Supporting Information

Holmes et al. 10.1073/pnas.1210657110

SI Materials and Methods

Fast Fourier Transforms. Fourier transforms (FTs) were performed using an established method (2) in which each amino acid in the sequence represents a discrete signal of either 1 (the hydrophobic residues F, A, M, I, L, Y, and V) or 0 (all other amino acids). The relative magnitudes of all frequencies (and thus all periodicities) of hydrophobic residues were then calculated using a fast FT. To obtain a high resolution, we calculated the magnitudes of 10,000 different frequencies between 1.0 and the number of amino acids in the sequence, and thus 10,000 different periodicities: period (units are amino acids) = sequence length/frequency. For each protein, we performed a fast FT on both the entire sequence and on all subsequent sequences of 65 residues.

Search for Proteins with *Streptomyces* Cytoskeletal Element-Like Coiled-Coil Repeats. We first screened the UniProt database with the MARCOIL program (3) to identify all sequences with at least one segment with a predicted coiled-coil probability of ≥0.5. Using an in-house C program and Perl scripts, these sequences were then subjected to a fast FT as above to calculate the hydrophobic periodicity of maximum strength in each window of 129 amino acids as above. Sequence segments were identified in which the mean strongest period, averaged over 65 consecutive such windows, was 51/14 (3.643) ± 0.001 residues, with a SD of ≤0.25. The positive segments were further screened by rejecting those that lacked at least one segment of at least 250 consecutive residues that contained no proline and fewer than 5% glycine residues.

Generation of KO Mutants. Mutant alleles of *scy* were generated in cosmid St8F4 (4) using PCR targeting (5). The apramycin resistance cassette (apramycin resistance gene and *oriT*) was PCR-amplified using appropriate primers: 8F4.kin.1 and 8F4.kin.2 for the *scy* mutant K110 and Scyknock_1 and Scyknock_2 for the *scy* mutant K111 (Table S3). The PCR cassettes were then introduced into cosmid St8F4 in BW25113 carrying pIJ790 (6) to generate St8F4/Δ*scy*(Δ28–381 amino acids)::*apr* and St8F4/Δ*scy*::*apr* mutants in *Escherichia coli*. After the mutant alleles were passaged through the *dcm-dam*- ET12567 strain (7) containing pUZ8002, they were introduced into *Streptomyces coelicolor* M145 by conjugation. The double-crossover exconjugants were tested for resistance to apramycin and sensitivity to kanamycin. To generate an unmarked *scy* mutant, we first removed the apramycin resistance cassette using the Flp recombinase of DH5α/BT340 (6) to generate St8F4/Δ*scy*::*scar* in *E. coli*. Then, we replaced the ampicillin resistance gene on the cosmid with the apramycin cassette and *oriT* to allow the delivery by conjugation and apramycin selection in *Streptomyces.* This cosmid was used to replace the Δ*scy*::*apr* in K111 with Δ*scy*::*scar* generating K112.

Spore counts were measured after collecting spores from confluent lawns of the WT and the *scy* mutant, K110, after 5 d of growth following the inoculation of ∼500 spores in soya flour medium (SFM).

Statistical Analysis of Hyphal Branching. Spores were inoculated onto cellophane membranes positioned on solid SFM medium and were incubated at 30 °C for 10–16 h. Samples taken from ∼1 cm^2 of the membrane were stained with WGA-Alexa488 and propidium iodide as described in the main text. Images were collected with a Zeiss AxioPlan 2ie microscope and a Zeiss AxioCam HRm CCD camera. Around 300 images of each bacterial strain were processed using custom-made analysis software, including noise reduction, background removal, and skeletonization, to produce a single pixel outline of the bacterial morphology. Algorithms then identified the branch points (B) and tip points (T), and measured the relevant lengths (L). New branch points were identified by finding short filaments of less than 1.5 μm (Fig. S3). The percent (%) distance was calculated using the following formula:

$$\%\ \text{distance} = 100\,\frac{L_T}{L_T + L_B}.$$

Plasmid Constructs Generated. ***Scy derivatives.*** pGS2 was created by first moving a 5.5-kb EcoRI-XhoI fragment of cosmid St8F4 (4) carrying *scy* into pET28a (Novagen) using its EcoRI-XhoI sites. The NdeI-KpnI fragment of this intermediate was replaced by a PCR product generated with primers, Scy-NdeI and Scy-KpnI, creating a construct, pGS2, where the start codon for *scy* overlapped with the NdeI site of pET28a, followed by the entire *scy* sequence and the downstream XhoI site of the chromosomal sequence. The protein product of pGS2 is His-tagged Scy.

To generate a pK48 for overproduction of Scy in *S. coelicolor*, we first moved the 4.5-kb XbaI-XhoI (blunted) fragment of pGS2 into the XbaI-HindIII (blunted) site of pCJW93, a multicopy vector (8). From this intermediate, we removed the small NdeI fragment generating pK48, a multicopy plasmid that replicates autonomously in *S. coelicolor* selectable with apramycin and produces His-Scy under the control of a thiostrepton-inducible promoter.

pK47 is a derivative of pIJ82, a vector that integrates at the ΦC31 *attB* site of the *S. coelicolor* chromosome and carries the hygromycin resistance gene (9). A 4.8-kb NruI-XhoI fragment carrying no more than *scy* with its promoter was blunt-ended and introduced into the EcoRV site of pIJ82, generating pK47.

To monitor Egfp-Scy, we generated pK56, a pIJ8660 (10) derivative carrying *egfp-scy* controlled by the native *scy* promoter. First, the annealed Linker1 and Linker2 primers were introduced into the XbaI-NdeI sites of pGS2, and a XbaI-BsrGI fragment containing *egfp* was then moved into this intermediate, generating an *egfp*-penta-glycine linker-*scy* translational fusion. From this construct, the NdeI-XhoI fragment carrying the *egfp-scy* fusion was moved into pEGFPC1 (Clontech) simply to generate an EcoRI site downstream of the *egfp-scy* casette. From this construct, the *egfp-scy* cassette could be lifted as an NdeI-EcoRI fragment. To generate a *mCherry-scy* cassette, we replaced the NdeI-BsrGI *egfp* fragment with an NdeI-BsrGI *mCherry* fragment from pBluescript-mCherry (gift of D. Widdick, John Innes Centre, Norwich, UK). The *scy* promoter fragment was generated by PCR using the primers Scyprom3 and Scyprom4, and it was introduced to pIJ8660 after digestion with BamHI and NdeI. We moved either the *egfp-scy* cassette generating pK56 or the *mCherry-scy* cassette generating pK57 to the NdeI-EcoRI sites of this plasmid. Both pK56 and pK57 are selectable with apramycin and integrate as a single copy into the ΦC31 *attB* site of the *S. coelicolor* chromosome, producing Egfp-Scy or mCherry-Scy from the native *scy* promoter in addition to the production of Scy at its normal chromosomal location.

pK52 contains the NdeI-EcoRI fragment of pK56 in pCJW93, a multicopy vector (8) producing a plasmid that can overproduce Egfp-Scy via induction by thiostrepton.

To monitor the effect of Scy overproduction on both DivIVA-Egfp and mCherry-Scy localizations, we could not use the existing pK48, pKF59, and pK57 together, because pK48 and pK57 both

use the apramycin resistance marker for selection. Instead of using pK57, we generated pK66 by introducing the 6.1-kb HindIII fragment of pK57 carrying *mCherry-scy* to the HindIII site of pMS82 (11) which is selectable by hygromycin and integrates at the ΦBT1 integration site on the chromosome.

DivIVA derivatives. pUT18c-DivIVA was generated by introducing *divIVA* as an XbaI-EcoRI fragment from a PCR product produced using the primers THDiv_F and THDiv_R that introduce the restriction sites XbaI and NdeI at the 5′-end, together with EcoRI at the 3′-end of *divIVA*. To generate pKT25-DivIVA, we moved the XbaI-EcoRI *divIVA* fragment from pUT18c-DivIVA to pKT25.

For overexpression and purification of His-DivIVA, the NdeI-EcoRI *divIVA* fragment of pUT18c-DivIVA was moved into pET28a to generate pK68.

FilP derivatives. pUT18c-FilP was constructed by introducing *filP* as an XbaI-EcoRI fragment from a PCR product produced using the primers THabpS_F and THabpS_R that introduce the restriction sites XbaI and NdeI at the 5′-end, together with EcoRI at the 3′-end of *filP*. To generate pKT25-FilP, we moved the XbaI-EcoRI *filP* fragment from pUT18c-FilP to pKT25.

For overexpression and purification of His-FilP, the NdeI-EcoRI *filP* fragment of pUT18c-FilP was moved into pET28a to generate pK70. For nontagged FilP production, the NdeI-EcoRI *filP* fragment of pUT18c-FilP was moved into pET21a to generate pK71.

The bacterial two-hybrid assays were performed according to the method of Karimova et al. (12).

CD Spectropolarimetry. After the purification of His-Scy, the protein concentration was determined by duplicate measurements using a 2-D Quant Kit (GE Healthcare). Far-UV CD spectra of the samples were recorded on an Applied Photophysics PiStar-180 spectropolarimeter. Duplicate samples of His-Scy (0.04 mg/mL) in 20 mM phosphate buffer (pH 8.0) were equilibrated at 25 °C in a thermostated quartz cell with a path length of 0.1 mm. CD data were recorded in the range of 190–260 nm at 1-nm intervals under nitrogen and averaged over 200,000 points with a 25-μs accumulation time. Slits were set at 4 nm. Spectral data were converted to residue molar ellipticity ([θ]) in deg $cm^2 \cdot dmol^{-1}$ and represent the average of 10 accumulations. The same samples of His-Scy were then preincubated for 1 h at room temperature in the presence of 50% (vol/vol) trifluoroethanol. CD spectra were recorded as described above, except that the protein concentration was 0.02 mg/mL and a 0.2-mm path length cell was used. All spectra were deconvoluted using CONTIN as implemented on the DICHROWEB Web site (http://dichroweb.cryst.bbk.ac.uk). The quality of fit was determined by the normalized rmsd parameter, which did not exceed 0.04 for any of the deconvolutions performed during this work.

In addition, we used the mean residue molar ellipticity at 222 nm ($[\theta]_{222}$) as a direct estimate of the proportion of the helicity, using the method of Gans et al. (13): The α-helix content is given by $[\theta]_{222}$ divided by the predicted ellipticity that would be obtained if all residues were in α-helical conformation. The latter is calculated as -40×10^{-3} (i.e., $1–4.6/n$), where n is the number of residues in the protein.

SEM. Cells were grown on solid SFM medium, and samples were taken by excising a piece of agar block containing a colony and attaching it to an aluminum stub. After quick freezing in liquid nitrogen, the sample was transferred onto the cryostage of a CT1500HF cryotransfer system attached to a Philips XL30 FEG scanning electron microscope. After sublimation of surface frost, the samples were sputter-coated with platinum for 2 min at 10 mA at a temperature colder than −110 °C and were then moved onto the cryostage in the main chamber of the microscope, held at approximately −140 °C, where they were viewed at 3 kV, and digital tagged image file format files were stored.

1. Flärdh K (2003) Essential role of DivIVA in polar growth and morphogenesis in *Streptomyces coelicolor* A3(2). *Mol Microbiol* 49(6):1523–1536.
2. McLachlan AD, Stewart M (1976) The 14-fold periodicity in alpha-tropomyosin and the interaction with actin. *J Mol Biol* 103(2):271–298.
3. Delorenzi M, Speed T (2002) An HMM model for coiled-coil domains and a comparison with PSSM-based predictions. *Bioinformatics* 18(4):617–625.
4. Redenbach M, et al. (1996) A set of ordered cosmids and a detailed genetic and physical map for the 8 Mb *Streptomyces coelicolor* A3(2) chromosome. *Mol Microbiol* 21(1):77–96.
5. Gust B, Challis GL, Fowler K, Kieser T, Chater KF (2003) PCR-targeted *Streptomyces* gene replacement identifies a protein domain needed for biosynthesis of the sesquiterpene soil odor geosmin. *Proc Natl Acad Sci USA* 100(4):1541–1546.
6. Datsenko KA, Wanner BL (2000) One-step inactivation of chromosomal genes in *Escherichia coli* K-12 using PCR products. *Proc Natl Acad Sci USA* 97(12):6640–6645.
7. MacNeil DJ, et al. (1992) Analysis of *Streptomyces avermitilis* genes required for avermectin biosynthesis utilizing a novel integration vector. *Gene* 111(1):61–68.
8. Wilkinson CJ, et al. (2002) Increasing the efficiency of heterologous promoters in actinomycetes. *J Mol Microbiol Biotechnol* 4(4):417–426.
9. Dalton KA, Thibessard A, Hunter JI, Kelemen GH (2007) A novel compartment, the 'subapical stem' of the aerial hyphae, is the location of a *sigN*-dependent, developmentally distinct transcription in *Streptomyces coelicolor*. *Mol Microbiol* 64(3):719–737.
10. Sun JH, Kelemen GH, Fernández-Abalos JM, Bibb MJ (1999) Green fluorescent protein as a reporter for spatial and temporal gene expression in *Streptomyces coelicolor* A3 (2). *Microbiology* 145(Pt 9):2221–2227.
11. Gregory MA, Till R, Smith MCM (2003) Integration site for *Streptomyces* phage phiBT1 and development of site-specific integrating vectors. *J Bacteriol* 185(17):5320–5323.
12. Karimova G, Pidoux J, Ullmann A, Ladant D (1998) A bacterial two-hybrid system based on a reconstituted signal transduction pathway. *Proc Natl Acad Sci USA* 95(10): 5752–5756.
13. Gans PJ, Lyu PC, Manning MC, Woody RW, Kallenbach NR (1991) The helix-coil transition in heterogeneous peptides with specific side-chain interactions: Theory and comparison with CD spectral data. *Biopolymers* 31(13):1605–1614.

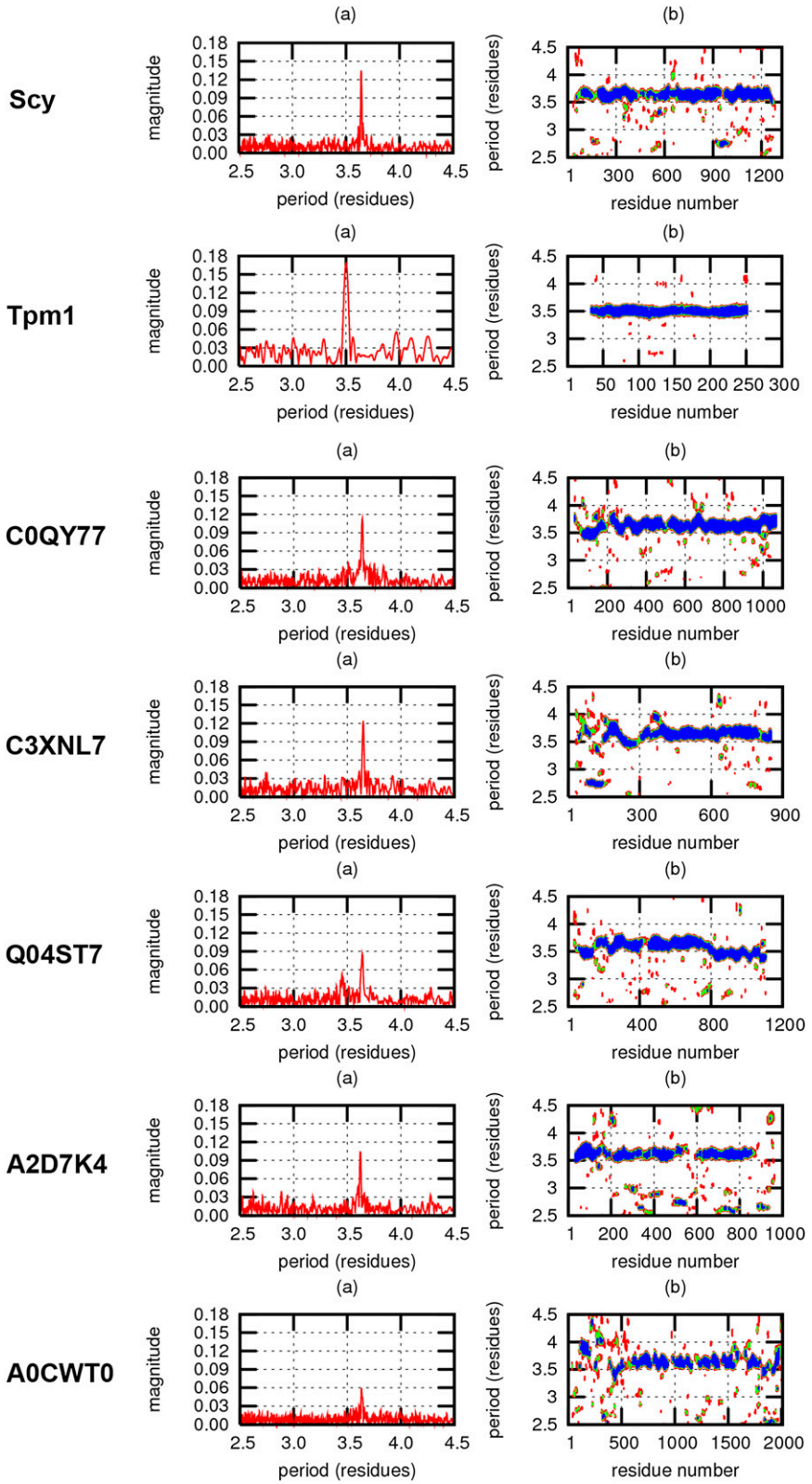

Fig. S1. Coiled-coil proteins with Scy-like repeat periodicity. Intensities of hydrophobic periodicities from fast FT of, respectively, a whole sequence (*A*) and sliding windows (*B*) for Scy, Q9L2C3 (*S. coelicolor*), Tpm1, P58772 (rabbit tropomyosin1), C0QY77 (*Brachyspira hyodysenteriae),* C3XNL7 (*Helicobacter wing-hamensis*), Q04ST7 (*Leptospira borgpetersenii*), A2D7K4 (*Trichomonas vaginalis*), and A0CWT0 (*Paramecium tetraurelia*), where UniProt numbers are shown. The noncanonical periodicity of Scy (3.643) contrasts with the 7/2 periodicity of the heptad repeat represented here by Tpm1 with a strong peak at 3.5. (*B*) *X* axis specifies the center of a window of 65 amino acids, and the *y* axis shows peaks in the periods of a fast FT of hydrophobic residues, using three contours defined as multiples (magnifications: red, 1.9×; green, 2.2×; blue, 2.5×) of the mean of all FT intensities (of any period) in the entire sequence. Only the first 1,100 residues of C0QY77 are shown.

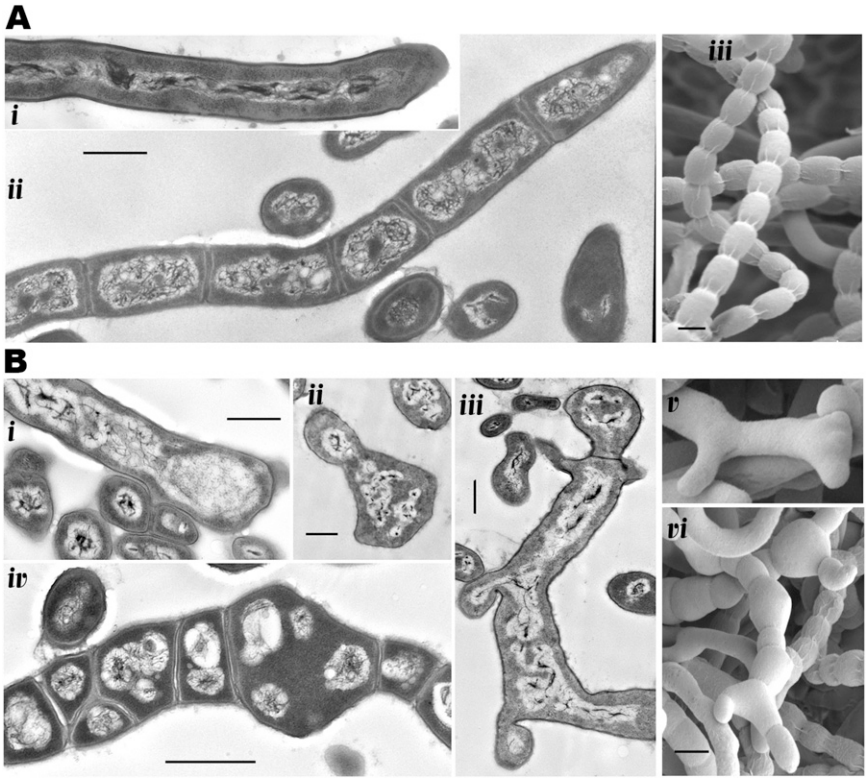

Fig. S2. Close-up of the hyphal geometry using EM. *S. coelicolor* WT (*A*) and the *scy* mutant, K110 (*B*), were grown on SFM medium for 44–72 h, and the hyphal geometry was assessed using transmission EM (*A*, *i* and *ii*; B, i, *ii*, *iii*, and *iv*) or SEM (*A*, *iii*; *B*, *v* and *vi*). Samples representing different stages of development are shown: hyphal filaments (*A*, *i* and *B*, *i*, *ii*, *iii*, and *v*), early spore chains (*A*, *ii* and *B*, *iv*), and mature spores (*A*, *iii* and *B*, *vi*). (Scale bars: *B*, *ii* and *iii*, 250 nm; all other panels, 500 nm.)

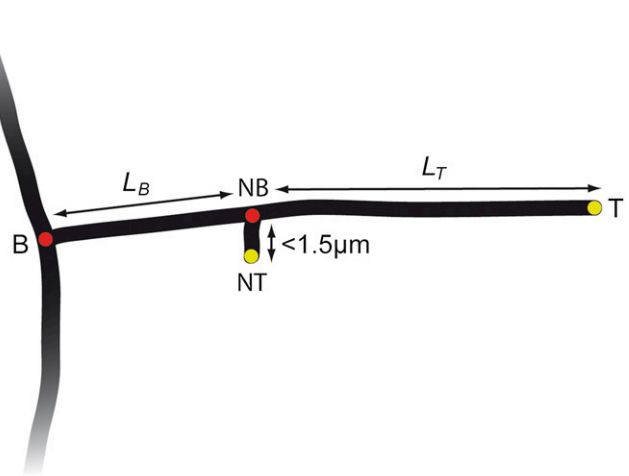

Fig. S3. Measuring the relative position of an emerging tip within an existing branch. The drawing represents the emergence of a new branch from an existing branch, where the new branches are defined as those with lengths <1.5 μm. The tips are marked with yellow dots, and the branchpoints are marked with red dots. The new tip (NT) and new branchpoint (NB) are distinguished from the existing tip (*T*) and the old branchpoint (*B*). The relative length (*L*) of a new branchpoint was calculated by the formula: % distance = 100 $\frac{L_T}{L_T + L_B}$.

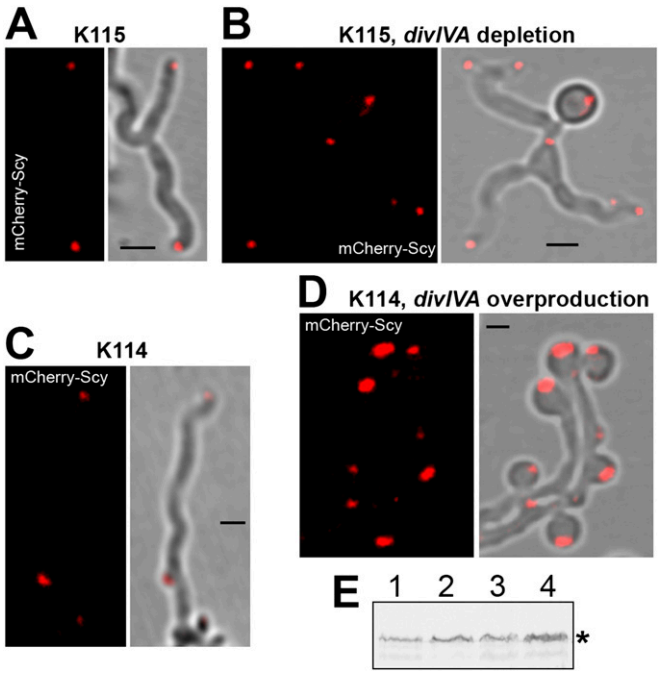

Fig. S4. Roles of Scy and DivIVA in establishing and maintaining polarized growth are closely linked. pK66 carrying mCherry-Scy was introduced into K115, which has a chromosomal *divIVA* deletion but carries a copy of *divIVA* under the thiostrepton-inducible promoter (1), and cells were grown in the presence of low levels of thiostrepton (0.1 μg/mL) for 16 h, followed by a further 3 h either in the presence (*A*) or absence (*B*) of thiostrepton. pK66 carrying mCherry-Scy was also introduced into K114, which can overproduce DivIVA in a thiostrepton-dependent manner, and cells were grown for an initial 16 h, followed by a further 3 h either in the absence (*C*) or presence (*D*) of thiostrepton (20 μg/mL). Images show the red channel for mCherry-Scy (*Left*), together with the overlayered view of the red channel in the bright-field view (*Right*). (*E*) Cell extracts from samples generated as in *C* and *D* were analyzed using SDS/PAGE, and the fluorescence emission of mCherry-Scy was monitored using a phosphoimager (Molecular Imager FX; BioRad). Samples were collected at 1 h (lanes 1 and 2) and 3 h (lanes 3 and 4) after thiostrepton induction. Uninduced (lanes 1 and 3) and thiostrepton-induced (lanes 2 and 4) samples are shown. mCherry-Scy is marked with an asterisk. (Scale bars: 1 μm.)

Table S1. Bacterial strains

Strain	Genotype or description	Source
S. coelicolor		
M145	SCP1$^-$ SCP2$^-$	(1)
K110	Δ*scy*(Δ28–381amino acids)::*apr* derivative of M145	This study
K111	Δ*scy*::*apr* derivative of M145	This study
K112	Δ*scy*::*scar* derivative of M145, generated from K111	This study
K114	M145 carrying pKF58	(2)
K115	ΔdivIVA::apr carrying pKF58, derivative of M145	(2)
E. coli		
DH5α	Cloning	Invitrogen
ET12567/pUZ8002	Transferring plasmids or cosmids from *E. coli* to *S. coelicolor* by conjugation	(3, 4)
BL21 (DE3)pLysS	Protein overproduction	Novagen
BW25113/ pIJ790	KO generation	(5)
DH5α/BT340	Unmarked KO generation	(5)
BTH101	Host for bacterial two-hybrid analysis	(6)

Table S2. Plasmid constructs

Plasmid	Genotype or description	Source
pET28a	Vector for protein overproduction	Novagen
pET21a	Vector for protein overproduction	Novagen
pIJ8660	This plasmid integrates as a single copy at the ΦC31 *attB* attachment site on the chromosome of *S. coelicolor*	(7)
pMS82	This plasmid integrates as a single copy at the ΦBT1 attachment site on the chromosome of *S. coelicolor*	(8)
pIJ82	This plasmid integrates as a single copy at the at the ΦC31 *attB* attachment site on the chromosome of *S. coelicolor*	(9)
pCJW93	Multicopy, autonomously replicates in *S. coelicolor*, carries thiostrepton-inducible promoter	(10)
pGS2	pET28a derivative for the production of His-Scy	This study
pKF58	This plasmid carries *divIVA* under the control of the thiostrepton-inducible promoter and integrates as a single copy at the at the ΦC31 *attB* attachment site on the chromosome of *S. coelicolor*	(2)
pKF59	pEGFP-1 derivative, produces DivIVA-Egfp fusion and integrates at the chromosomal *divIVA* site, generating both DivIVA-Egfp and native DivIVA	(2)
pKF41	pIJ8660 derivative, produces FtsZ-Egfp fusion	(11)
pK47	pIJ82 derivative carrying *scy* with its promoter on a 4.8-kb NruI-XhoI fragment of *S. coelicolor*	This study
pK48	Derivative of the multicopy plasmid, pCJW93, carrying *scy* under the control of a thiostrepton-inducible promoter	This study
pK52	Derivative of the multicopy plasmid, pCJW93, carrying *egfp-scy* under the control of a thiostrepton-inducible promoter	This study
pK56	Egfp-Scy fusion under the control of native P*scy* in the integrative plasmid pIJ8660	This study
pK57	N-terminal mCherry-Scy fusion under the control of native P*scy* in the integrative plasmid pIJ8660	This study
pK66	pMS82 derivative, produces mCherry-Scy under the control of native P*scy*, integrating into the ΦBT1 attachment site in the chromosome	This study
pK68	pET28a derivative for the production of His-DivIVA	This study
pK70	pET28a derivative for the production of His-FilP	This study
pK71	pET21a derivative for the production of nontagged FilP	This study
pUT18c	Vector carrying the T18 fragment for the bacterial two-hybrid system	Euromedex
pKT25	Vector carrying the T25 fragment for the bacterial two-hybrid system	Euromedex
pUT18c-zip	T18 translational fusion to the leucin zipper of GCN4	(6)
pKT25-zip	T25 translational fusion to the leucin zipper of GCN4	(6)
pUT18c-Scy	T18 translational fusion to Scy	(12)
pKT25-Scy	T25 translational fusion to Scy	(12)
pUT18c-DivIVA	T18 translational fusion to DivIVA	This study
pKT25-DivIVA	T25 translational fusion to DivIVA	This study
pUT18c-FilP	T18 translational fusion to FilP	This study
pKT25-FilP	T25 translational fusion to FilP	This study
pUTc-ScyII	T18 translational fusion to ScyII	Gift of D. Jakimowicz*
pUTc-ScyIII	T18 translational fusion to ScyIII	Gift of D. Jakimowicz*
pUTc-ScyIV	T18 translational fusion to ScyIV	Gift of D. Jakimowicz*

*Institute of Immunology, Wroclaw, Poland.

1. Kieser T, Bibb MJ, Buttner MJ, Chater KF, Hopwood DA (2000) *Practical Streptomyces Genetics* (The John Innes Foundation, Norwich, UK).
2. Flardh K (2003) Essential role of DivIVA in polar growth and morphogenesis in *Streptomyces coelicolor* A3(2). *Mol Microbiol* 49(6):1523–1536.
3. MacNeil DJ, et al. (1992) Analysis of *Streptomyces avermitilis* genes required for avermectin biosynthesis utilizing a novel integration vector. *Gene* 111(1):61–68.
4. Paget MS, Chamberlin L, Atrih A, Foster SJ, Buttner MJ (1999) Evidence that the extracytoplasmic function sigma factor sigmaE is required for normal cell wall structure in *Streptomyces coelicolor* A3(2). *J Bacteriol* 181(1):204–211.
5. Datsenko KA, Wanner BL (2000) One-step inactivation of chromosomal genes in *Escherichia coli* K-12 using PCR products. *Proc Natl Acad Sci USA* 97(12):6640–6645.
6. Karimova G, Pidoux J, Ullmann A, Ladant D (1998) A bacterial two-hybrid system based on a reconstituted signal transduction pathway. *Proc Natl Acad Sci USA* 95(10):5752–5756.
7. Sun JH, Kelemen GH, Fernandez-Abalos JM, Bibb MJ (1999) Green fluorescent protein as a reporter for spatial and temporal gene expression in *Streptomyces coelicolor* A3(2). *Microbiology* 145:2221–2227.
8. Gregory MA, Till R, Smith MCM (2003) Integration site for streptomyces phage phi BT1 and development of site-specific integrating vectors. *J Bacteriol* 185(17):5320–5323.
9. Dalton KA, Thibessard A, Hunter JI, Kelemen GH (2007) A novel compartment, the "subapical stem" of the aerial hyphae, is the location of a *sigN*-dependent, developmentally distinct transcription in *Streptomyces coelicolor*. *Mol Microbiol* 64(3):719–737.
10. Wilkinson CJ, et al. (2002) Increasing the efficiency of heterologous promoters in actinomycetes. *J Mol Microbiol Biotech* 4(4):417–426.
11. Grantcharova N, Lustig U, Flardh K (2005) Dynamics of FtsZ assembly during sporulation in *Streptomyces coelicolor* A3(2). *J Bacteriol* 187(9):3227–3237.
12. Walshaw J, Gillespie MD, Kelemen GH (2010) A novel coiled-coil repeat variant in a class of bacterial cytoskeletal proteins. *J Struct Biol* 170(2):202–215.

Table S3. Oligonucleotides

Name	Oligonucleotide sequence
8F4.kin.1	CCTCTCTCGGTTCGAGGCCGAGATGAAGCGGCTGAAGACCTGTAGGCTGGAGCTGCTTC
8F4.kin.2	TCCTCGGTGGCCGCCTTCGTGGTCCGCTTGGCGTCCTCCGATTCCGGGGATCCGTCGACC
Scyknock_1	GAAGATTTGCGACCAGGGGACGGATGGGACCGCGCAGTGATTCCGGGGATCCGTCGACC
Scyknock_2	GCCCACCGTCGCTCCGGCCTTCACCCCGTTGTCCTTCGCTGTAGGCTGGAGCTGCTTC
Linker1	CTAGACTGATGTACAACGGCGGCGGCGGCGG
Linker2	TACCGCCGCCGCCGCCGTTGTACATCAGT
scyNde1	ACCGCCATATGCGGGGCTACGAGAGCCAGGAGC
scyKpn2	CGCGTTGCGCAGCAACTGCTCG
scyprom3-Nde	ACCGCCATATGCGCGGTCCCATCCGTCCC
scyprom4-Bam	CTGGAGGATCCCGTACGCGTTCTGTACGACGAGC
THDiv_F	GGATCATCTAGAGCATATGCCGTTGACCCCCGAGGACG
THDiv_R	GGATCAGAATTCTCAGTTGTCGTCCTCGTCGATCAGGAACC
THAbpS_F:	GGATCATCTAGAGCATATGAGCGACACTTCCCCCTACG
THAbpS_R:	GGATCAGAATTCTCAGCGGGACTGCTGGGCCG
AbpS_Nde_Cterm	GGATCACATATGGCGGGACTGCTGGGCCGGGACC
EGFPLINKER1	GATCCTCTAGACATATGGGCGGCGGCGGCGG
EGFPLINKER2	TACCGCCGCCGCCGCCCATATGTCTAGAG